



## Probabilistic study on the relationship between the residual deformation and the accumulated plastic deformation by an earthquake

J. Iyama<sup>(1)</sup>

<sup>(1)</sup> Associate Professor, The University of Tokyo, iyama@arch1.t.u-tokyo.ac.jp

### Abstract

The residual deformation after an earthquake could be an index of structural damage to a building, if the relationship between the residual deformation ( $d_r$ ) and the accumulated (total) plastic deformation ( $d_t$ ), were obtained. For this purpose, in this paper, the probabilistic relationship between residual deformation and accumulated plastic deformation of a perfectly elastic-plastic single-degree-of-freedom oscillator is discussed.

In the previous study, the author showed that the conditional probability of the residual deformation ( $d_r$ ) given the number of plastic excursions ( $n$ ) and the accumulated plastic deformation ( $d_t$ ) is almost a normal distribution with an average of zero and a standard deviation of  $d_t$  over the square root of  $n$ . Using this finding, the probability density function (PDF) of the residual deformation ( $d_r$ ) can be formulated with the joint PDF of  $n$  and  $d_t$ . Moreover, if one can assume that  $n$  and  $d_t$  were statistically independent, it could be represented with each PDFs of  $d_t$  and  $d_r$ .

Inversely, in this paper, the conditional PDF of  $d_t$  given  $d_r$  was derived, which would make it possible to estimate accumulated structural damage (i.e.,  $d_t$ ) to a building from the observed residual deformation (i.e.,  $d_r$ ) after an earthquake.

In order to validate the derived equations of the conditional PDF of  $d_t$  given  $d_r$ , dynamic response analysis using a large number of pseudo ground motions simulated by the inverse Fourier transform.

The analysis result showed that each PDF of the number of plastic excursion ( $n$ ) and the accumulated plastic deformation ( $d_t$ ) can be approximated by the gamma distribution. From these approximated PDF for  $n$  and  $d_t$  and the derived equations, with the assumption that  $n$  and  $d_t$  are statistically independent, the conditional PDF of  $d_t$  given  $d_r$  was calculated and compared to the histogram of  $d_r$  calculated from the analysis result. The estimated PDF succeeded to capture the tendency that larger  $d_t$  would be estimated when larger  $d_r$  was observed, which was seen in the analytical results. The estimated mean and standard deviation of  $d_t$  given  $d_r$  also showed a reasonable agreement with the analytical results.

From the above discussion, it can be concluded that, it is impossible to estimate  $d_t$  (i.e. structural damage) only from  $d_r$ , however, if the prior distributions of  $d_t$  and  $n$  is known, it would be possible to improve the estimation accuracy of  $d_t$  using the proposed equations and the observed  $d_r$ .

*Keywords: Residual deformation; Conditional probability; Bayes' theorem; Damage estimation*



## 1. Introduction

For fast recovery after an earthquake disaster, it is important to determine if a damaged building is safe enough to use it continuously or not as soon as possible. However, it is difficult to determine, in a quantitative manner, how much structural damage is received by a building, because most of the structural members are covered by interior and exterior walls and ceilings and could not be investigated nor seen without destructing them.

In a guideline for post-earthquake damage inspection [1] used in Japan, the structural damage of a building is presumed from the observed residual story drift which it is easy to measure. However, the residual deformation does not directly represent the accumulated (total) plastic deformation nor the structural damage. In addition, shown in many literatures [2, 3, 4, 5] on the relationship between the residual deformation and the accumulated plastic deformation, one can say that the residual deformation has a very large dispersion and that it may be difficult to handle it as a deterministic value.

The author considers that the residual deformation should be treated as a probabilistic value and has been studied on the probabilistic characteristics of the residual deformation of a perfectly elastic-plastic single-degree-of-freedom (SDOF) oscillator. In the previous paper [6], the author showed that the conditional probability distribution of the residual deformation,  $d_r$ , given the number of plastic excursions,  $n$ , and the accumulated (total) plastic deformation,  $d_t$ , is almost a normal distribution with an average of zero and a standard deviation of  $d_t$  over the square root of  $n$ .

Using this knowledge, it is possible to estimate the probability density function (PDF) of  $d_r$  from the observed  $d_r$ , which may enable one to use  $d_r$  as an index of structural damage. This paper shows and validates this method through dynamic response analysis using a number of simulated ground motions.

## 2. Theoretical relationship between residual and total plastic deformations

### 2.1 Analysis oscillator model

This paper discusses the dynamic behavior of a single-degree-of-freedom (SDOF) model with an elastic-perfectly plastic characteristics as shown in Fig. 1. The plastic deformation in the  $i$ -th plastic excursion during an earthquake is denoted as  $d_i$ . The residual and total plastic deformation after the earthquake are denoted as  $d_r$  and  $d_t$ , respectively, which are represented as,

$$d_r = \sum_{i=1}^n d_i, d_t = \sum_{i=1}^n |d_i| \quad (1)$$

### 2.2 Relationship between residual and total plastic deformation

The author showed in a previous paper [1] that the probabilistic distribution function (PDF) of the residual deformation  $f(d_r|d_t, n)$  under a given total plastic deformation,  $d_t$ , and a number of yielding occurrence,  $n$ , can be modeled as a normal distribution with a mean of 0 and a standard deviation of  $d_t/\sqrt{n}$ , which is represented as,

$$f(d_r|d_t, n) \sim N\left(0, \frac{d_t}{\sqrt{n}}\right) = \frac{\sqrt{n}}{\sqrt{2\pi}d_t} \exp\left(-\frac{nd_r^2}{2d_t^2}\right) \quad (2)$$

Using this equation, the conditional PDF of  $d_t$  given  $d_r$  can be written as:

$$f(d_t|d_r) = \frac{\int f(d_r|d_t, n) \cdot f(d_t, n) dn}{f(d_r)} \quad (3)$$

This equation means that in order to calculate  $f(d_t|d_r)$ , a simultaneous PDF,  $f(d_t, n)$ , should be known. In addition, if one can assume  $d_t$  and  $n$  are probabilistically independent, it can be represented as a product of the PDFs of  $d_t$  and  $n$ , as follows.

$$f(d_t, n) = f(d_t) \cdot f(n) \tag{4}$$

Therefore, it is possible to estimate the PDF of total damage (i.e.  $d_t$ ) under the condition of observed residual deformation (i.e.  $d_r$ ) from Eq. (3),  $f(d_t)$ , and  $f(n)$ .

Here, we assume that  $f(d_t)$ , and  $f(n)$  can be approximated with gamma functions:

$$f(d_t, n) = f(d_t) \cdot f(n) = G[d_t, k_t, \theta_t] \cdot G[n, k_n, \theta_n] \tag{5}$$

Where  $G[x, k, \theta]$  denotes the gamma distribution with the shape factor,  $k$ , and the scale factor,  $\theta$ . These factors are calculated from the mean and variance of  $d_t$  or  $n$ . By using the gamma distribution, the integration in Eq. (3) can be erased and the equation can be represented as follows:

$$f(d_t|d_r) \sim \frac{G[d_t, k_t - 1, \theta_t]}{\left(\frac{1}{\theta_n} + \frac{d_r^2}{2d_t^2}\right)^{k_n + \frac{1}{2}}} \tag{6}$$

The right hand side of this equation is not normalized, though, the shape of the conditional PDF can be obtained without numerical integrations.

### 3. Validation using simulated ground motions

In order to validate the derived equation (Eq. (6)) of the conditional PDF of  $d_t$  given  $d_r$ , in this chapter, dynamic response analysis using a large number of pseudo ground motions simulated by the inverse Fourier transform is performed.

#### 3.1 Analysis model

An SDOF system with elastic-perfectly plastic hysteric characteristics, as previously shown in Fig. 1, is used for dynamic response analysis. The parameters of the model are the natural period,  $T$ , and the yield strength,  $Q_y$ . For  $T$ , values of 0.5s, 1.0s and 1.5s are used.  $Q_y$  is determined as  $Q_y = D_s Q_e$ , where  $Q_e$  is the maximum restoring force of the elastic model, and for  $D_s$ , values of 0.2, 0.4 and 0.6 are used.

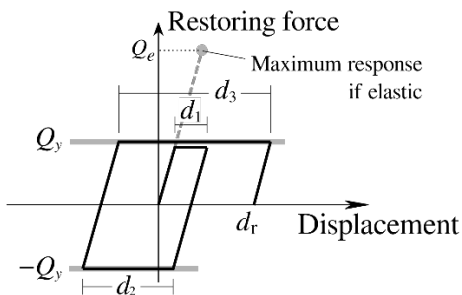


Fig. 1 – Restoring force characteristics

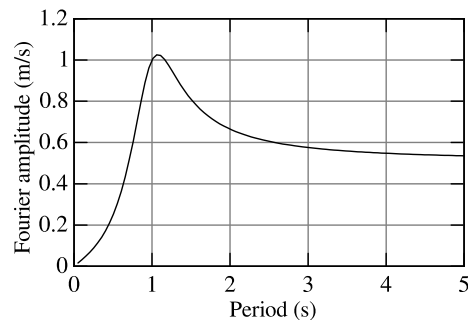


Fig. 2 – Kanai-Tajimi spectrum[7]

### 3.2 Input ground motions

In this chapter, simulated ground motions by the inverse Fourier transform are used for the analysis. Kanai-Tajimi spectrum [7], shown in Fig. 2, is used for the amplitude (absolute) components of the Fourier spectrum, where the predominant period  $T_d = 1.0s$  and the shape factor  $h_g = 0.3$  as proposed in [7]. The phase (argument) components for the Fourier spectrum are determined so that the phase difference spectrum would follow the “near-field” type, “intermediate” type, and “oceanic” type spectrum defined in literature [8]. The examples of simulated ground motions for these three types are shown in Fig. 3. The “near-field” type ground motion has a large energy input in a short time, while the “oceanic” type has a longer vibration with smaller acceleration amplitude.

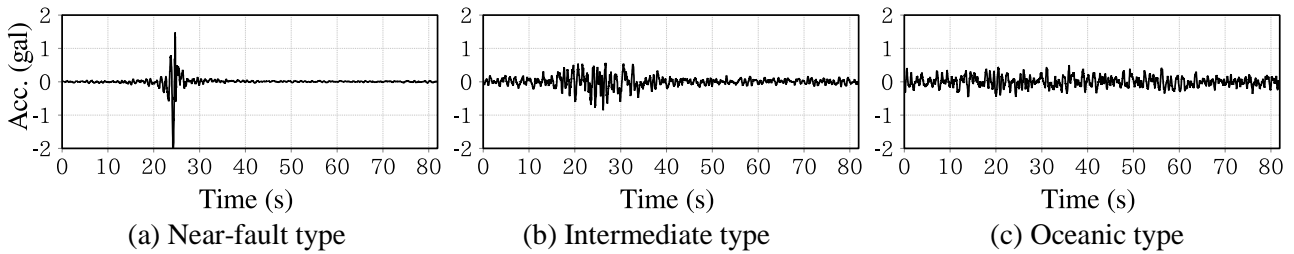


Fig. 3 – Examples of simulated ground motions

### 3.3 Probability density function of the total plastic deformation and number of plastic occurrence

Fig. 4 shows the PDFs of the number of plastic occurrence,  $n$ , the PDF of the total plastic deformation,  $d_t$ , and the joint PDF of  $n$  and  $d_t$  for various phase types and natural periods obtained from the dynamic response analysis. In this figure, only the cases of  $D_s = 0.4$  are shown due to limitations of space but it was confirmed that there are no large different tendency in other cases than  $D_s = 0.4$  are observed.

Each figure (e.g., Fig. 4(a1)) consists of three types of graphs. The top graph shows the PDF of  $n$ . In this graph, the bars represent the histogram of  $n$  obtained from the dynamic response analysis results, which are normalized so that the area is 1.0. In this graph, approximated gamma distribution (i.e.  $G[n, k_n, \theta_n]$ ) is also shown with line, where the shape factor,  $k_n$ , and the scale factor,  $\theta_n$ , are calculated from the mean and variance of  $n$  obtained from the dynamic response analysis.

The right graph in vertical orientation shows the PDF of  $d_t$ . Similarly to the top graph, the bars represent the histogram of  $d_t$ , and the line represents the approximated gamma distribution, i.e.  $G[d_t, k_t, \theta_t]$ .

The center graph shows the contour of the joint PDF of  $n$  and  $d_t$ , where the darker area represents the larger probability.

In the top and right graphs, it is shown that each PDF of  $n$  and  $d_t$  can be approximated as a gamma distribution. On the while, in the center graph, there is positive or negative correlation observed between  $n$  and  $d_t$ , which varies according to natural periods, phase types and also  $d_s$ 's. However, the correlation is not significantly large especially for the cases of intermediate-type ground motions. From these results, it can be presumed that Eq. (5) which assumes the statistical independence between  $n$  and  $d_t$  is satisfied in a certain accuracy.

However, it should be noted that, in this simulation, the Fourier amplitude spectrum of the ground motions, the natural period and the yield strength of the system are assumed to be constant, respectively, and therefore that the total input energy (i.e.,  $d_t$ ) is almost constant. This may be the reason why the observed correlation was small. In actual cases where earthquakes must have a very large variation in the strength, more correlation between  $n$  and  $d_t$  may be observed and the accuracy of Eq. (5) and (6) should be re-validated.

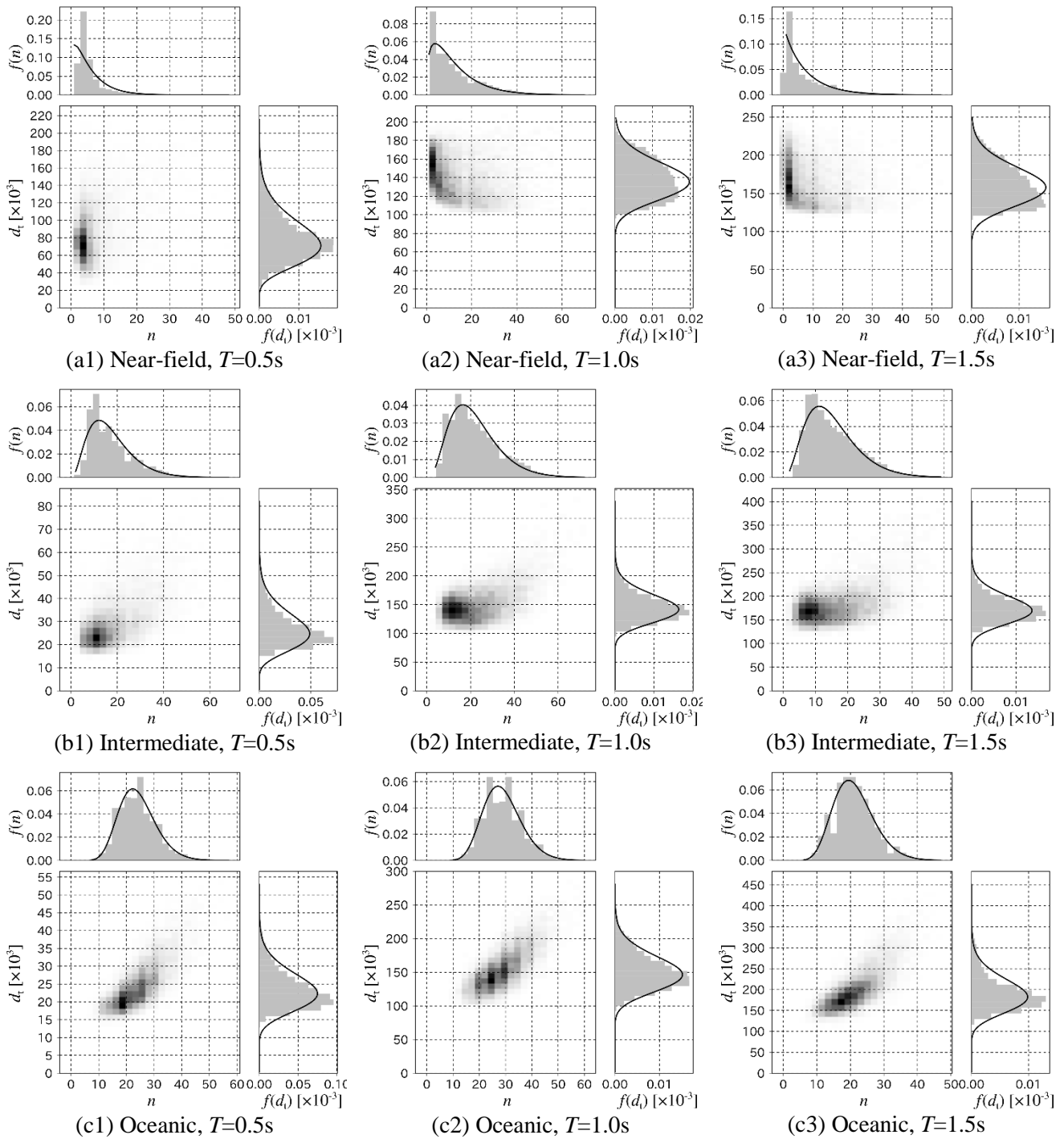


Fig. 4 –Joint PDF of  $n$  and  $d_t$ . ( $D_s = 0.4$ )



### 3.4 Estimated PDF of $d_t$ under given $d_r$

By using the estimated joint PDF calculated from the gamma distributions shown in Fig. 2, it is possible to estimate the PDF of  $d_t$  given  $d_r$  from Eq. (6). The comparison between the estimated PDF of  $d_t$  given  $d_r$  and the actual PDF obtained from dynamic response analysis is shown in Fig. 5.

The bar in each graph shows the histogram of  $d_t$  where  $d_r$  is in a certain range shown in each graph. The lower graph has larger  $d_r$ . The range of  $d_r$  is chosen so that the number of response analysis,  $N$ , shown in each graph is 200. It is observed that the peak of the histogram moves rightward as  $d_r$  is getting larger. This means that larger  $d_r$  might imply larger  $d_t$ , which can be easily presumed.

The line in each graph shows the estimated PDF of  $d_t$  under  $d_r$  calculated with Eq. (6) and gamma distributions shown in Fig. 4, where the center value of the  $d_r$  range shown in the figure is used for the estimation. For the cases of intermediate and oceanic type ground motions (Fig. 5(b1) to (c3)), it is observed that the estimated curves agree the histograms in a good accuracy. For the cases of near-field type ground motions (Fig. 5(a1) to (a3)), the estimated curves capture the trend that larger  $d_t$  is expected in the case of larger  $d_r$ , but the accuracy is worse. It should be noted that, as shown in the bottom graph in Fig. 5(b1) for example, large probability density is estimated in the range of  $d_t < d_r$ , which is improbable. This defect should be improved in the future study.

For the purpose to show the accuracy for all cases, the mean and standard deviation of the actual and estimated  $f(d_t|d_r)$  are compared in Fig. 6. “●” and “□” represent the mean,  $\mu$ , and the mean plus standard deviation,  $\mu + \sigma$ , respectively, of the estimated  $f(d_t|d_r)$ . While, the solid line and dashed line represent the mean and the mean plus standard deviation, respectively, of the histogram obtained from dynamic analysis. One can read the accuracy by comparing “●” and the solid line, and “□” and the dashed line.

As shown previously in Fig. 5, the estimation for the near-field type ground motions does not show a good accuracy. But in other cases, the estimated values are approximately agrees the analysis result in a certain accuracy. It is presumed that this method can be applicable in many cases except the extreme case of near-field ground motions.

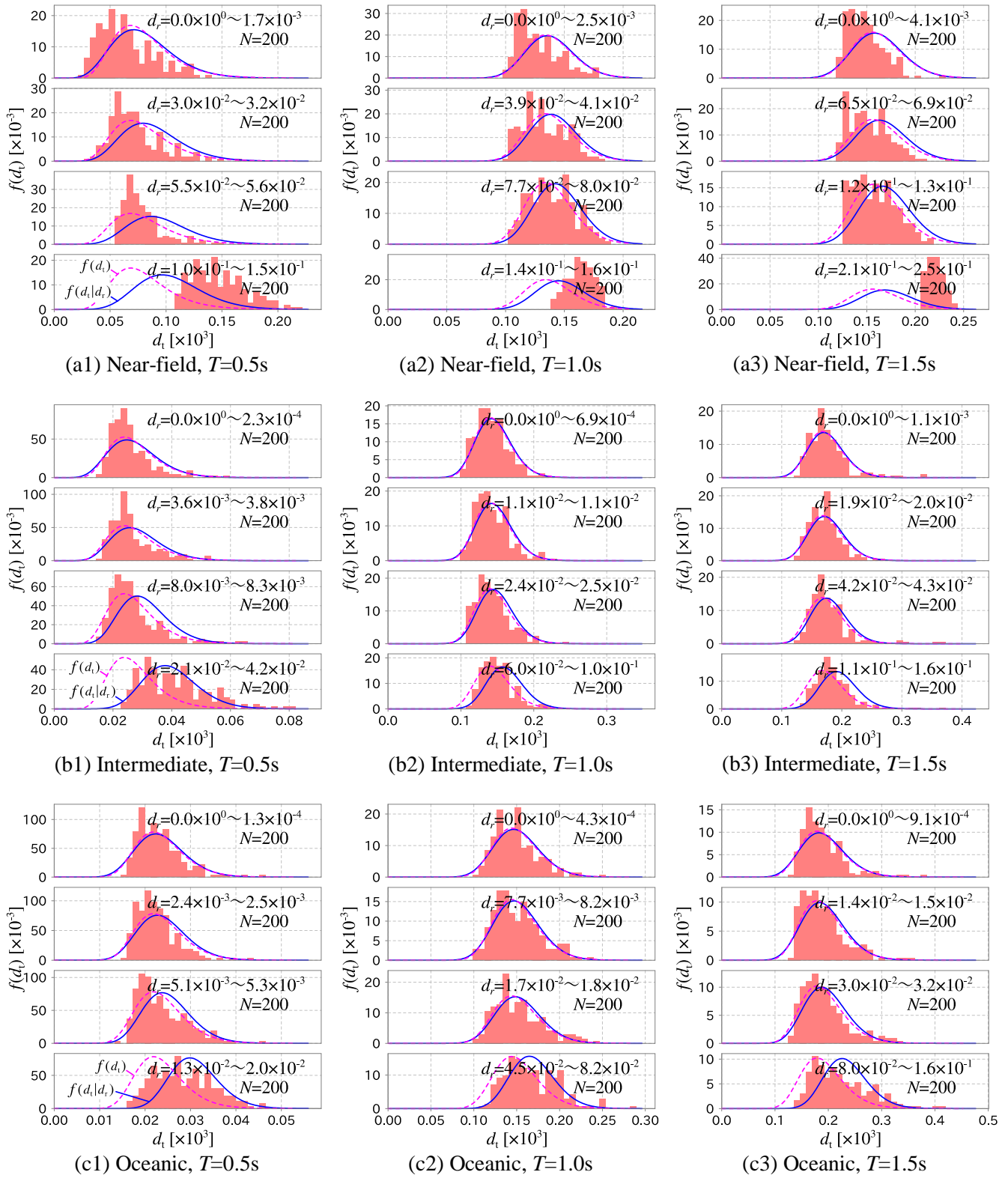


Fig. 5 –Conditional PDF of  $d_t$  under  $d_r$

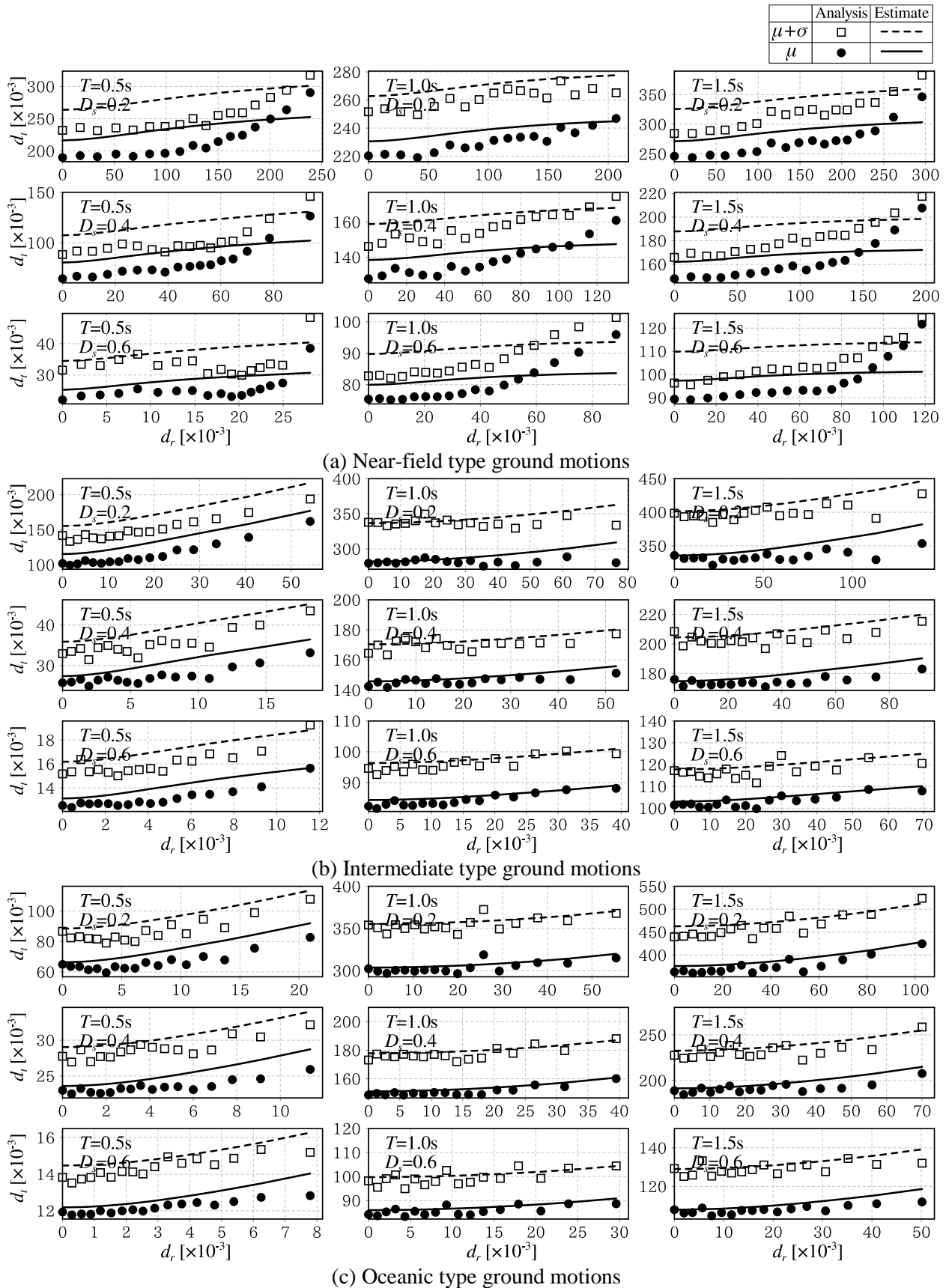


Fig. 6 – Mean and standard deviation of conditional PDF of  $d_t$  under  $d_r$



## 4. Conclusion

The authors showed in a previous paper that the PDF of residual deformation of an oscillator after an earthquake,  $d_r$ , could be considered to be a normal distribution with a standard deviation of  $d_t/\sqrt{n}$ , where  $d_t$  is the total plastic deformation and  $n$  is the number of yielding during the earthquake, by assuming “random walk” hypothesis. In this paper, using this knowledge and Bayes' theorem, the conditional PDF of  $d_t$  under a condition of  $d_r$ ,  $f(d_t|d_r)$ , was formulated as a function of the joint PDF of  $n$  and  $d_t$ ,  $f(n, d_t)$ . This equation can be used for the purpose of estimation of total structural damage (i.e.  $d_t$ ) from an observed residual deformation (i.e.  $d_r$ ).

Dynamic response analysis of a number of simulated and recorded ground motions were performed to validate this method. The conditional PDF of  $d_t$  given  $d_r$ , obtained from this analysis, showed a similar trend to the estimated conditional PDF,  $f(d_t|d_r)$ , by the obtained equation. The means and standard deviations from the dynamic analysis also showed a reasonable agreement with the estimated values.

In this discussions, it can be concluded that, though it is impossible to estimate  $d_t$  only from  $d_r$ , it is possible to improve the estimation accuracy of  $d_t$  using the proposed equations. However, the accuracy of this method is presumed to be affected by the accuracy of the approximated joint PDF,  $f(n, d_t)$ , as well as that of the accuracy of the random-walk hypothesis, which is affected by the yield strength of the building and the time-frequency characteristics of input ground motions. For more detailed validation of this method, analysis using a large number of actual ground motions and a more realistic structural model should be performed in a future study.

## References

- [1] Japan Building Disaster Prevention Association (2015): Guidelines for Post-earthquake Damage Evaluation and Rehabilitation of Buildings and Houses (Japanese).
- [2] MacRae GA, Kawashima K (1997): Post-earthquake residual displacements of bilinear oscillators. *Earthquake Engineering and Structural Dynamics*. 26:7, 701-716.
- [3] Kawashima K, MacRae GA, Hoshikuma J, Nagaya K (1998): Residual Displacement Response Spectrum. *J. Structural Engineering*, ASCE. 124:5. 523-530, 1998.
- [4] Akiyama H, Takahashi M (1998): Residual Deformation of Flexible-Stiff Mixed Shear-Type Multi-Story Frames under Earthquakes. *Summaries of Technical Papers of Annual Meeting, AIJ*. B-2: 397-398. (In Japanese)
- [5] Christopoulos C, Pampanin S, Priestley MJN (2003): Performance-based seismic response of frame structures including residual deformations. Part 1: Single-degree of freedom systems. *J. Earthquake Engineering*. 7:1 97-118.
- [6] Iyama J (2012) : Estimation of probability distribution of the residual displacement of bilinear SDOF systems after earthquake ground motions. *15th WCEE*, Lisbon, Portugal.
- [7] Tajimi H (1960): A statistical method of determining the maximum response of a building structure during an earthquake. *2nd WCEE*, Tokyo, 781-797.
- [8] Iwata Y, Kuwamura H (2003): Study on input earthquake ground motions for seismic performance evaluation of steel buildings. Part 2. Representative spectra of recorded ground motions. *Proc. Architectural Research Meetings, Kanto Chapter, AIJ*, 133-136. (In Japanese)